Cooperativity in the Binding of Echinomycin to DNA Fragments Containing Closely Spaced CpG Sites†

Christian Bailly,‡,§ François Hamy,|| and Michael J. Waring*,§

Department of Pharmacology, University of Cambridge, Tennis Court Road, Cambridge CB2 1QJ, U.K., Institut de Recherches sur le Cancer, INSERM U124, Place de Verdun, 59045 Lille Cedex, France, and Ciba-Geigy Ltd., Pharmaceutical Division, Basel 4002, Switzerland

Received July 24, 1995; Revised Manuscript Received October 3, 1995⊗

ABSTRACT: Quantitative footprinting has been used to investigate cooperative binding of the antitumor antibiotic echinomycin to DNA fragments containing closely spaced CpG steps. The sequences of the designed DNA fragments contained two pairs of strong echinomycin binding sites: a pair of ACGT sites together with an ACGT site and a TCGA site, either directly adjacent or separated by two or four A·T base pairs. The results demonstrate that the binding of echinomycin to the sequences ACGTACGT and TCGAACGT is highly cooperative. The extent of cooperativity depends on the nature of the sequences clamped by the antibiotic and diminishes as the distance between the binding sites is increased. Various methods of extracting the information necessary to establish cooperativity have been compared. Beyond the specific interest in echinomycin−DNA interaction, the present quantitative footprinting study provides a model that may be generally applicable for designing investigations into cooperativity in drug−DNA recognition.

Echinomycin (Figure 1) is a cyclic octadepsipeptide antibiotic that selectively inhibits DNA-directed RNA synthesis in a variety of biological systems (Waring, 1979, 1993). Its antitumor activity is believed to result from its capacity to bind tightly to DNA by a mechanism of bis-intercalation (Waring & Wakelin, 1974). Footprinting studies have established that echinomycin binds preferentially to sites surrounding CpG steps in DNA (Low et al., 1984; Van Dyke & Dervan, 1984). Its sequence selectivity is apparently mediated by the formation of three hydrogen bonds between the alanine residues of the ligand and the N3 and 2-amino groups of the guanosine nucleotides in the recognition site. Recent studies from our laboratory have emphasized the determinant role of the exocyclic 2-amino group of guanine exposed in the minor groove for sequence-specific recognition between echinomycin (as well as several other antibiotics) and DNA (Marchand et al., 1992; Bailly et al., 1993; Bailly & Waring, 1995a).

The three-dimensional structures of numerous complexes between a quinoxaline antibiotic and an oligonucleotide have been solved at atomic resolution by X-ray crystallography or NMR spectroscopy (Table 1). Studies on 1:1 echinomycin−DNA complexes have revealed the exact orientation of the antibiotic molecule inserted around a CpG step. Structural studies of 2:1 echinomycin−oligonucleotide complexes have shed light on the effect of flanking sequences on echinomycin−CpG recognition. It has been shown that two

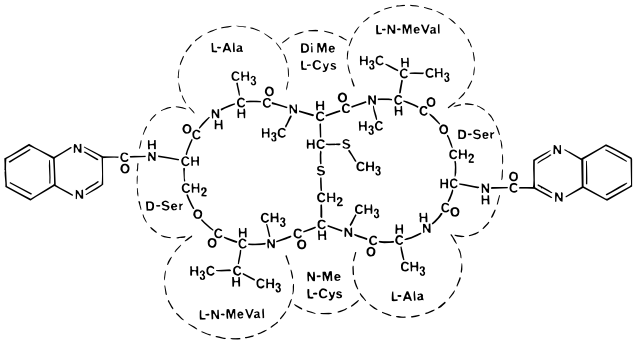

FIGURE 1: Structure of echinomycin.

Table 1: Structures of Oligonucleotide−Quinoxaline Antibiotic Complexes Determined to Atomic Resolution

drug−DNA complex	reference
triostin A−CGTACG	Wang et al. (1984)
echinomycin−CGTACG	Ughetto et al. (1985)
triostin A−GCGTACGC	Quigley et al. (1986)
echinomycin−ACGT	Gao and Patel (1988)
echinomycin−TCGA	Gao and Patel (1988)
echinomycin−GCGC	Gao and Patel (1989)
echinomycin−CCGC	Gao and Patel (1989)
echinomycin−AAACGTTT	Leroy et al. (1992)
echinomycin−CCAAACGTTTGG	Leroy et al. (1992)
echinomycin−ACGTACGT	Gilbert and Feigon (1989)
echinomycin−TCGATCGA	Gilbert and Feigon (1991)
echinomycin−ACGTATACGT	Gilbert and Feigon (1992)
triostin A−GACGTC	Addess and Feigon (1994a)
triostin A−GGACITCC	Addess and Feigon (1994b)
triostin A−ACGTACGT	Addess and Feigon (1994c)

echinomycin molecules bind cooperatively to two ACGT sites either juxtaposed (ACGTACGT) (Gilbert & Feigon, 1991) or spaced by two additional A·T base pairs (ACGTATACGT) (Gilbert & Feigon, 1992). By contrast, there is no cooperativity between juxtaposed TCGA sites: two echinomycin molecules clamp independently around each CpG step in the sequence TCGATCGA (Gilbert & Feigon,

† This work was done under the support of research grants from the INSERM and the ARC (to C.B.), and from the Wellcome Trust, CRC, AICR, and the Sir Halley Stewart Trust (to M. J. W.). Portions of the research were presented at the 39th meeting of the Biophysical Society (San Francisco, February 1995).

* Address correspondence to this author.
‡ INSERM U124.
§ University of Cambridge.
|| Ciba-Geigy.

⊗ Abstract published in *Advance ACS Abstracts,* December 15, 1995.

0006-2960/96/0435-1150$12.00/0 © 1996 American Chemical Society

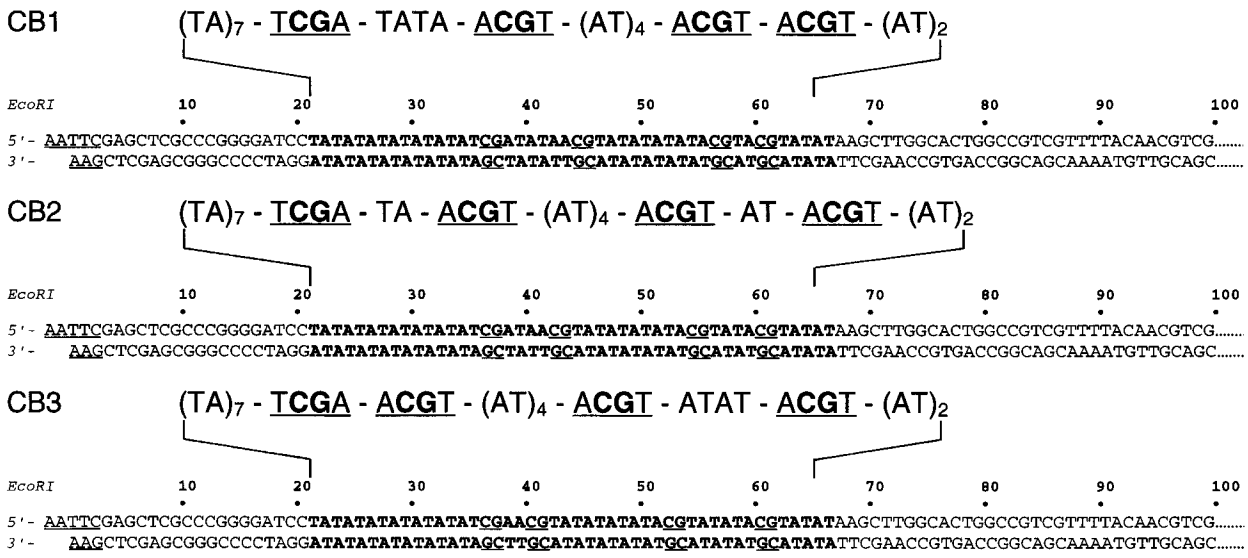

FIGURE 2: Sequences of the DNA fragments containing the inserts CB1, CB2, and CB3 (bold characters). In each case the plasmid was double digested with *Eco*RI plus *Pvu*II and then 3′- or 5′-end labeled at the *Eco*RI site (underlined).

1991). Cooperative binding of echinomycin and related drugs to DNA was also evidenced in early equilibrium binding studies (Lee & Waring, 1978; Fox et al., 1982; Shafer & Waring, 1982) and more recently in footprinting studies (Sayers & Waring, 1993; Bailly & Waring, 1995b) which showed that echinomycin binds much more strongly to the CpG steps in the sequences ACGACGT and ACGACGG than to sequences containing an isolated CpG dinucleotide step. These several observations have prompted the conclusion that the stability of echinomycin−DNA complexes depends to a considerable extent on the sequence at and adjacent to the binding site.

We have sought to examine in greater detail the cooperativity of binding of echinomycin to DNA by measuring the strength of binding to DNA fragments containing closely spaced CpG steps. A series of 52-mer oligonucleotides were cloned into pUC12, each containing two pairs of classical echinomycin binding sites (ACGT and TCGA) in direct juxtaposition or spaced by two or four A·T base pairs (Figure 2). Footprinting experiments using DNase I as cleaving agent were performed to investigate binding of the antibiotic to these sites at nucleotide resolution. Quantitative analysis of the footprinting patterns was undertaken to provide an accurate estimate of the relative drug occupancy at each CpG step and thus to permit direct determination of the influence of a neighboring site on the recognition of a particular CpG step by echinomycin. The results establish unambiguously that the binding of echinomycin to DNA can be highly cooperative and that the extent of cooperativity depends on the nature of the sequences clamped by the antibiotic. Beyond the specific interest for echinomycin−DNA interaction, the present study illustrates the usefulness of the quantitative footprinting methodology as a sensitive means of detecting cooperativity in drug−DNA recognition.

MATERIALS AND METHODS

Antibiotic. Echinomycin was obtained from Parke-Davis (New Jersey) and dissolved to a concentration of 80 μM in 10 mM Tris-HCl, pH 7.0, 10 mM NaCl containing 40% (v/v) methanol. The stock solution was diluted to working concentrations with appropriate volumes of 10 mM Tris-HCl, pH 7.0, 10 mM NaCl, and methanol so as to yield a final methanol concentration of 10% (v/v) in the footprinting reactions. Methanol-containing buffer was used for the drug-free control samples. Under our conditions methanol is known not to affect deoxyribonuclease activity (Low et al., 1984; Portugal et al., 1988). An extinction coefficient of 11 500 M^{-1} cm^{-1} was used to determine echinomycin concentration from absorbance measurements at 325 nm (Waring, 1979).

Chemicals and Biochemicals. Ammonium persulfate, Tris-base [Tris(hydroxymethyl)amino methane], acrylamide, bisacrylamide, ultrapure urea, boric acid, tetramethylethylenediamine, and dimethyl sulfate were from BDH. Formic acid, piperidine, hydrazine, and formamide were from Aldrich Chemicals, Inc. Photographic requisites were from Kodak. Bromophenol blue and xylene cyanole were from Sigma Chemical Co. Bovine pancreatic deoxyribonuclease I (DNase I, EC 3.1.21.1, Sigma Chemical Co.) was stored as a 7200 units/mL solution in 20 mM NaCl, 2 mM $MgCl_2$, 2 mM $MnCl_2$, pH 7.3, at −20 °C and was freshly diluted to the desired concentration immediately prior to use. Restriction endonucleases were purchased from Boehringer Mannheim and used according to the supplier's recommended protocol in the activity buffer provided. Alkaline phosphatase, AMV reverse transcriptase, and T4 polynucleotide kinase were from Pharmacia. α-[^{32}P]dATP and γ-[^{32}P]ATP (6000 Ci/mmol) were purchased from New England Nuclear. Unlabeled forms of ATP and dATP (ultrapure grade) were purchased from Pharmacia. All other chemicals were analytical grade reagents, and all solutions were prepared by using doubly deionized, 0.22 μm Millipore-filtered water.

DNA Purification and Labeling. Plasmids were isolated from *Escherichia coli* by a standard sodium dodecyl sulfate−sodium hydroxide lysis procedure and purified by banding in CsCl−ethidium bromide gradients. Ethidium was removed by several isopropanol extractions followed by exhaustive dialysis against Tris-EDTA buffer. The purified plasmid was then precipitated and resuspended in appropriate buffer prior to digestion by the restriction enzymes. To clone the AT-rich inserts (Figure 2), a synthetic 52-mer oligonucleotide and its complement were mixed at a 1:1 ratio,

heated to 70 °C, and slowly cooled to form the duplex. The sequences of the oligonucleotides were designed so that they could be cloned between the *Hin*dIII and *Bam*HI sites of the pUC12 vector. The vector plasmid pUC12 was double digested with *Bam*HI and *Hin*dIII prior to ligation with the insert. The resulting plasmid construct (pCB1, pCB2, and pCB3) was transformed into *E. coli* TG1 cells. The DNA fragment for footprinting was prepared by 3′-[^{32}P]-end labeling of the *Eco*RI−*Pvu*II double digest of pCB plasmid using α-[^{32}P]dATP (6000 Ci/mmol) and AMV reverse transcriptase or by 5′-[^{32}P]-end labeling of the *Eco*RI/alkaline phosphatase treated plasmid using γ-[^{32}P]ATP (6000 Ci/mmol) and T4 polynucleotide kinase followed by treatment with *Pvu*II. The digestion products were separated on an 8% polyacrylamide gel under non-denaturing conditions in TBE buffer (89 mM Tris-borate, pH 8.3, 1 mM EDTA). After autoradiography, the band corresponding to the 168 base pair fragment was excised, crushed, and soaked in elution buffer (500 mM ammonium acetate, 10 mM magnesium acetate) overnight at 37 °C. This suspension was filtered through a Millipore 0.22 μm filter and the DNA was precipitated with ethanol. Following washing with 70% ethanol and vacuum drying of the precipitate, the labeled DNA was resuspended in 10 mM Tris adjusted to pH 7.0 containing 10 mM NaCl.

DNase I Footprinting. DNase I experiments were performed essentially according to the original protocol (Low et al., 1984). Reactions were conducted in a total volume of 10 μL. Samples (3 μL) of the labeled DNA fragment were incubated with 5 μL of the buffer solution containing the desired echinomycin concentration. After 60 min of incubation at 37 °C to ensure equilibration of the binding reaction, the digestion was initiated by the addition of 2 μL of the endonuclease solution whose concentration had been adjusted to limit the digestion to less than 30% of the starting material so as to minimize the incidence of multiple cuts in any strand ("single-hit" kinetic conditions). Optimal enzyme dilutions were established in preliminary calibration experiments. Typically, DNase I experiments included 0.01 unit of enzyme/mL, 20 mM NaCl, 2 mM $MgCl_2$, 2 mM $MnCl_2$, pH 7.3. At the end of the reaction time (routinely 3 min at room temperature), the digestion was stopped by freeze-drying. After lyophilization each sample was washed once with 50 μL of deionized water then lyophilized again prior to resuspending in 4 μL of an 80% formamide solution containing tracking dyes (purchased from Sigma). Samples were generally electrophoresed immediately, but they can be stored (at 4 °C for up to 24 h) prior to resuspending in the dye solution. Samples were heated at 90 °C for 4 min and chilled in ice for 4 min prior to electrophoresis.

Electrophoresis and Autoradiography. Cleavage products resulting from the DNase I reactions were resolved by polyacrylamide gel electrophoresis under denaturing conditions (0.3 mm thick, 8% acrylamide containing 8 M urea). Electrophoresis was continued until the bromophenol blue marker had run out of the gel (about 2.5 h at 60 W, 1600 V in TBE buffer, BRL sequencers model S2). Gels were soaked in 10% acetic acid for 15 min, transferred to Whatman 3MM paper, dried under vacuum at 80 °C, and subjected to autoradiography at −70 °C with an intensifying screen. Exposure times of the X-ray films (Fuji R-X) were adjusted according to the number of counts per lane loaded on each individual gel (usually 24 h).

Densitometry. To achieve an accurate and sensitive densitometric analysis of the footprinting data, we tested two independent methods. In the first approach, we employed phosphor screen storage technology (Johnston et al., 1990), which permits rapid and sensitive quantitative analysis and claims to provide a linear response over an extremely wide range of band densities. In this case, the ImageQuant software from Molecular Dynamics was used to measure the radioactivity profiles of the gel lanes and to quantify band intensities. In the second approach, bands on an autoradiograph (i.e., a photographic film exposed for a critical time carefully adjusted to provide optimal sensitivity) were quantitated by a nonlinear least-squares program using the software package GELTRAK specifically developed for quantitative footprinting (Smith & Thomas, 1990). Unlike ImageQuant, GELTRAK allows the operator to fit each band on the autoradiograph with a Gaussian line shape and thus permits accurate measurement of band intensities, particularly of closely spaced bands. In any event, no important differences between the results obtained from the two procedures were noticed. By virtue of its speed and convenience, the phosphor screen imaging system is the method of choice.

A Molecular Dynamics 425E PhosphorImager was used to collect the data from storage screens exposed to dried gels overnight at room temperature. Base line-corrected scans were analyzed by integrating all of the densities between two selected boundaries using ImageQuant version 3.3 software. Footprinting data are presented in the form $\ln(f_a) - \ln(f_c)$ representing the differential cleavage at each bond relative to that in the control (f_a is the fractional cleavage at any bond in the presence of the drug, and f_c is the fractional cleavage of the same bond in the control). The results are displayed on a logarithmic scale for the sake of convenience; positive values indicate enhanced cleavage whereas negative values indicate blockage. Each resolved band on the phosphorimage was assigned to a particular bond within the DNA fragment by comparison of its position relative to the sequencing standards generated by treatment of the DNA with dimethyl sulfate (G), formic acid (G + A) or hydrazine (T + C) followed by piperidine-induced cleavage at the modified bases.

Data Reduction. Peak areas were stored on a disk as an ASCII file and subsequently transferred into standard spreadsheet programs (Cricket Graph and Kaleidagraph) using a Macintosh personal computer. The final data set consisted of 55 band positions (positions 20−74) for each strand of each insert fragment. At a given nucleotide position, data were obtained for a total of 17 echinomycin concentrations. Peak areas were determined in duplicate and were averaged. Over 10 000 individual peak areas were thus determined in our analysis. The procedure used to derive the footprinting plots was based on previous methods (Ward et al., 1987; Dabrowiak & Goodisman, 1989; Sayers & Waring, 1993). In the first stage, peak areas were corrected for slight differences in the total amount of DNA loaded per lane by multiplying the peak area by a specific correction factor. This factor is determined from a total cut plot, i.e., a plot of the sum of all band intensities in a given lane *vs* the total echinomycin concentration. These individual corrections yield the "corrected" or "normalized" band intensities which are used to construct the footprinting plots. In the present case, each total cut plot was a line of near-zero

slope. Footprinting plots were then constructed by plotting R *vs* c, where c is the ligand concentration. The relative band intensity R corresponds to the ratio I_c/I_o, where I_c is the intensity of the band at a given concentration c, and I_o is the intensity of the same band in the control lane, i.e., in the absence of the antibiotic. IC_{50} values were obtained by fitting the experimental data in each footprinting plot using a nonlinear iterative curve fitting a sigmoid function

$$Y = A - \frac{(A - B)(10^x)}{(10^x) + (10^C)} \qquad \text{(eq 1, fit 1)}$$

$$Y = A - \frac{(A - B)(10^x)^D}{(10^x)^D + (10^C)^D} \qquad \text{(eq 2, fit 2)}$$

where A is the top plateau (R_{max}), B is the bottom plateau (R_{min}), C is the log IC_{50} ($-pIC_{50}$), and D is the slope. The fitting was performed using the software package Kaleidagraph running on a Macintosh computer.

In preliminary tests it was established that the reproducibility of determination of IC_{50} values from independent experiments was generally better than ±5%, i.e., comparable to the range of variation observed when using different methods of curve fitting (see below). In a few instances where the top plateau (R_{max}) was not well defined, it was set to 1.0, which is the limiting value corresponding to nil footprinting effect which must apply at antibiotic concentrations tending to zero. Here again, tests to investigate the effect of choosing R_{max} within the range actually observed at other bonds produced no differences in C_{50} that exceeded the confidence limits derived from the curve-fitting procedure [Sayers and Waring (1993) and unpublished observations].

The following equation was used to calculate the F value for a comparison of the fits provided by the two models:

$$F = \frac{(SS_1 - SS_2)/(SS_2/df_2)}{(df_2 - df_2)}$$

where SS_1 and SS_2 are the sum of squares of the residuals from fit 1 and fit 2, respectively, and df_1 and df_2 are the degrees of freedom of fit 1 and fit 2, respectively. The degrees of freedom were calculated as the number of echinomycin concentrations used to construct the footprinting plots, from which was subtracted the number of floating parameters used in the curve fit (i.e., three for fit 1 and four for fit 2). The F test indicated that fit 2 was sometimes better than fit 1, i.e., that the inclusion of an additional parameter improved the goodness of fit of the regression curve to the data set. However, the IC_{50} values determined from fit 1 or fit 2 were very little different (the maximum variation observed was 4.2%).

Another procedure employed to estimate the relative affinity of the antibiotic for defined sites consisted of using the first four or five concentrations in each footprinting plot, determining the initial slope by fitting them to a straight line, and then dividing the slope of the line by the y-intercept. The more negative the slope, the higher the binding constant of the antibiotic at that site (Dabrowiak et al., 1989; Stankus et al., 1992; Shubsda et al., 1994).

RESULTS

Sequence-Specific Recognition. The three DNA fragments (168 bp) containing the insert sequences CB1, CB2, and CB3 (Figure 2) were 3′- or 5′-end labeled at the *Eco*RI site on one or the other of the complementary strands. A series of mixtures containing one of the three ^{32}P-labeled DNA fragments and a large distribution of echinomycin concentrations was prepared and, after 1 h of incubation at 37 °C to establish equilibrium (Fox et al., 1981), the DNA in these samples was exposed to the nicking activity of DNase I. Echinomycin concentrations varying from 0.1 to 30 μM were chosen so as to generate solutions in which the fractional occupancy of DNA binding sites varied from a few percent to near 100%. Typical autoradiographs obtained with each insert are shown in Figure 3. The rate of cleavage by the enzyme is subject to considerable modulation through local binding of echinomycin. Although visual inspection of the gels will suffice to ascertain that the antibiotic binds specifically to the CpG steps, it is necessary to conduct an accurate densitometric analysis of autoradiograms from each footprint titration in order to construct binding isotherms whence the strength of binding can be determined.

For both strands of each DNA fragment, we have examined the footprinting patterns over the complete range of echinomycin concentrations up to 30 μM so as to determine the full concentration-dependence profile at all CpG sites and at AT sequences proximal and distal to the binding sites. The densitometric analyses were naturally limited to regions where the bands were sufficiently well resolved to permit unambiguous quantification. However, thanks to the high quality of the original polyacrylamide gels, the entire region of the inserts could be accurately analysed on both the 3′- and 5′-labeled fragments. The corresponding differential cleavage plots in Figure 4 show the exact location of the footprints (negative values) as well as regions where the cleavage by the nuclease is enhanced in the presence of the antibiotic (positive values). The plots reveal unambiguously that the sites of reduced DNase I cleavage (presumptive drug-binding sites) are located around the ACGT and TCGA sites, as expected, with the customary 2−3 bp stagger in the 5′ → 3′ direction due to binding of the peptide ring in the minor groove. Adjoining the CpG-containing binding sites, there are sequences which are rendered hypersensitive to DNase I attack in the presence of the drug. Enhancement of DNase I cutting occurs characteristically at the AT tracts flanking the ACGT and TCGA binding sites. When those binding sites are separated by four A·T base pairs, the two footprints are well defined. For example, the two adjacent protected regions in CB1 around positions 38 and 46 coincide very well with the TCGA and ACGT sites, respectively. Similarly, the two ACGT sites in CB3 which are separated by four A·T bp give rise to two well-defined footprints clearly identifiable on both strands of the insert sequence. The two footprints tend to merge when the binding sites are directly juxtaposed or separated by only two A·T bp. In such cases, a broad region of DNase I protection covering the two binding sites is observed, but it remains possible to distinguish those two sites. For example, the binding of echinomycin to the two ACGT sites in CB1 (positions 56−59 and 60−63) yields a large footprint encompassing the two tetranucleotides, but at moderate echinomycin concentrations the bimodal shape of the differential cleavage plots at this position is properly accounted for by the presence of two individual sites.

Cooperative Binding of Echinomycin to GpC-Containing Sites. To determine precisely whether (and to what extent)

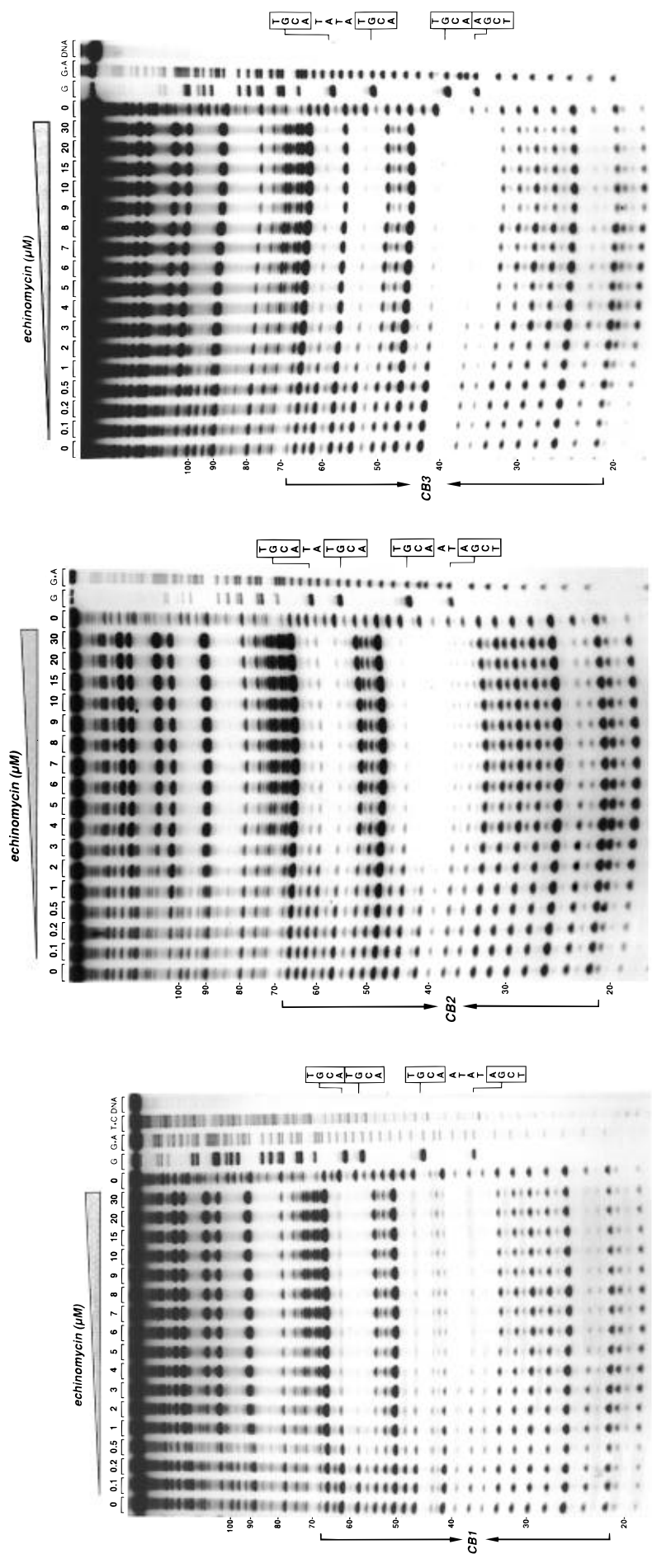

FIGURE 3: DNase I footprinting of echinomycin on the 168 bp DNA fragments containing the inserts CB1, CB2, and CB3 (from left to right). For each experiment, the duplex DNA was 5′-end labeled at the *Eco*RI site with γ-[^{32}P]ATP in the presence of T4 polynucleotide kinase. The cleavage products were resolved on an 8% polyacrylamide gel containing 8 M urea. Control lanes (marked 0) show the products resulting from limited DNase I digestion of the DNA fragment in the absence of the antibiotic. Lanes labeled G, G + A, and T + C show the products resulting from the dimethyl sulfate/piperidine, formic acid/piperidine, and hydrazine/piperidine reactions and indicate the location of guanine, purine, and pyrimidine residues, respectively, within the sequence. The lane marked "DNA" contained the ^{32}P-labeled DNA alone, incubated without antibiotic or enzyme; this sample serves as a control to assess background nicking of the DNA. The remaining lanes show the products of DNase I digestion of each fragment in the presence of increasing concentrations of echinomycin (expressed as micromolar). Numbers at the left side of the gels refer to the numbering scheme used in Figure 2. The sequences on the right side show the location of the ACGT and TCGA sites to which echinomycin binds.

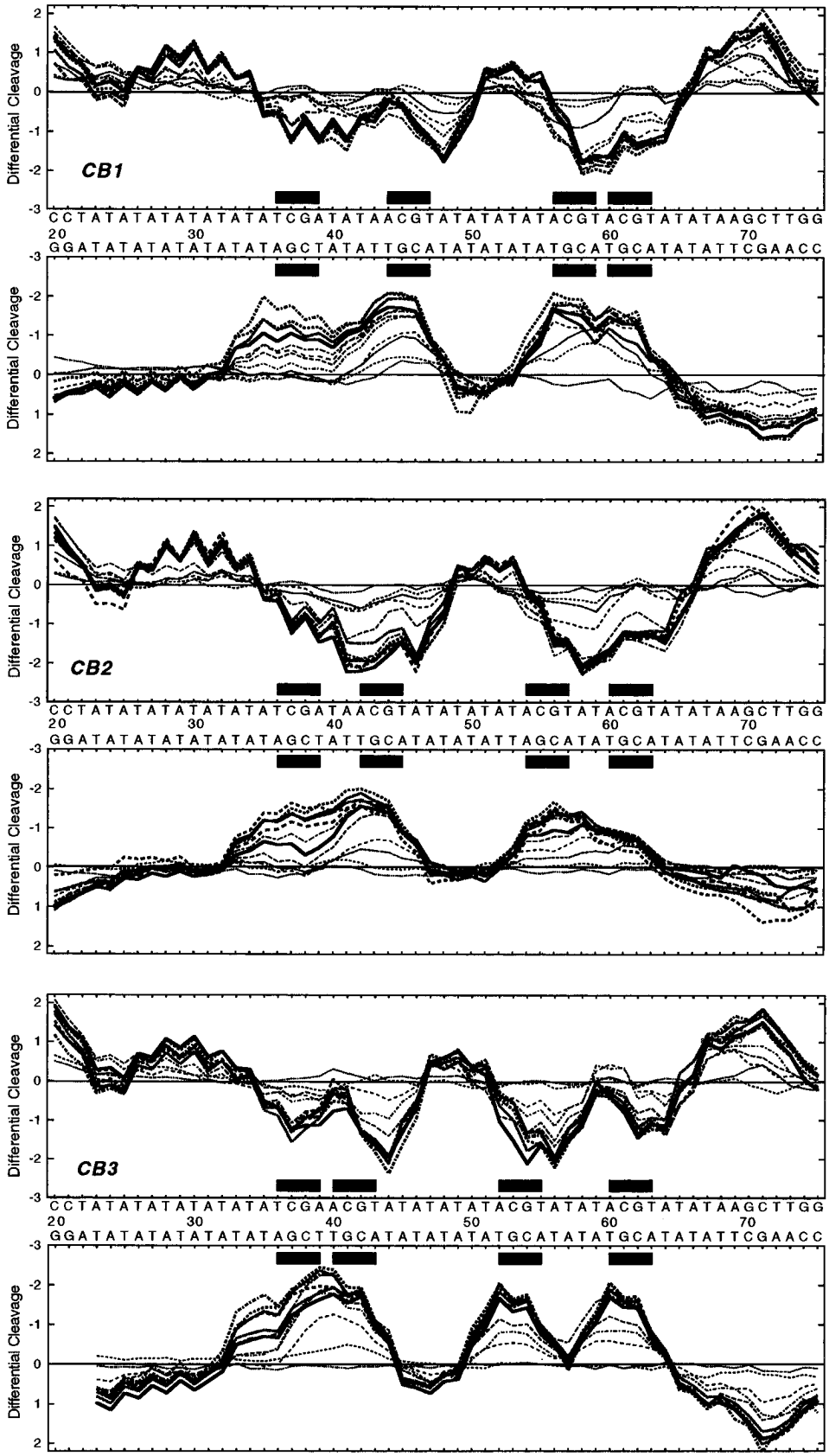

FIGURE 4: Differential cleavage plots comparing the susceptibility of the DNA containing the sequences CB1, CB2, and CB3 to cutting by DNase I in the presence of various concentrations of echinomycin (0.1−30 μM). The panel above each lettered sequence shows differential cleavage of the 5′-labeled strand, the lower panel shows that of the complementary 3′-labeled strand. The ordinate scales for the two strands are inverted, so that deviation of points toward the lettered sequence (negative values) corresponds to a ligand-protected site and deviation away (positive values) represents enhanced cleavage. Vertical scales are in units of $\ln(f_a) - \ln(f_c)$, where f_a is the fractional cleavage at any bond in the presence of the drug and f_c is the fractional cleavage of the same bond in the control, given a closely similar extent of digestion in each case. The lines drawn represent a three-bond running average of individual data points, calculated by averaging the value of $\ln(f_a) - \ln(f_c)$ at any bond with those of its two nearest neighbors. The results are displayed on a logarithmic scale for the sake of convenience. The filled rectangles show the positions of the ACGT and TCGA sites.

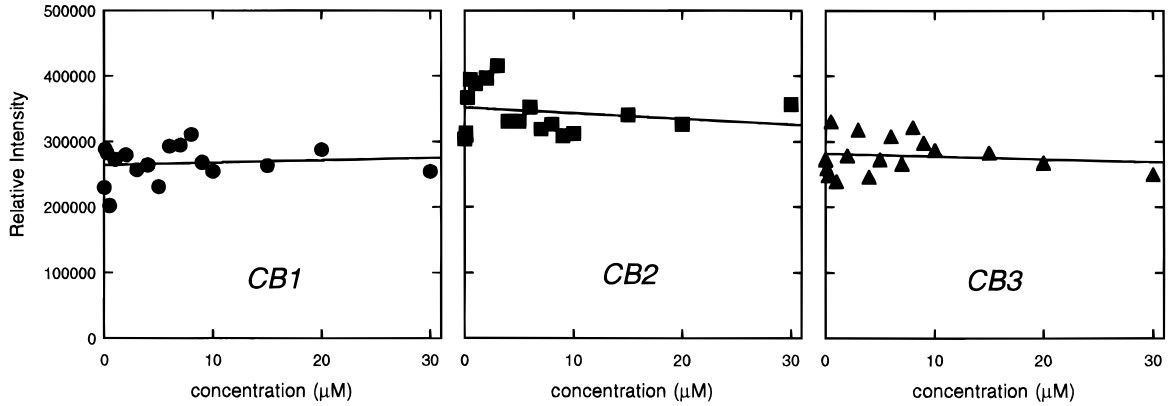

FIGURE 5: "Total cut" plots showing the summed cleavage of the 168 bp DNA fragments CB1, CB2, and CB3 as a function of echinomycin concentration. Intensities on the *y*-axis, representing the summed intensities of all bands in a given gel lane, are expressed in arbitrary units.

the binding of echinomycin to the designed DNA fragment is cooperative, we considered the variation of band intensities as a function of antibiotic concentration. Prior to using band intensities to derive the so-called footprint plots (Dabrowiak & Goodisman, 1989), the raw data were normalized to a common base by summing all band intensities in a given lane on the autoradiogram. Typical plots of the total intensity in each lane as a function of echinomycin concentration are shown in Figure 5. In each case, the best fit to the summed data points is a linear plot with slope close to zero, indicating that the total amount of cleavage on the restriction fragment remains practically constant. Decreases in cleavage intensity within the CpG-containing echinomycin binding sites are roughly compensated by increases in cleavage where the drug does not bind, i.e., at $(AT)_n$ sequences. The total cut plots allow band intensities to be corrected for gel-loading and errors in digestion time via multiplication of each band intensity by a correction factor equal to the ratio between the fitted line and the experimental point for a given echinomycin concentration in the total cut plot. Corrected band intensities thus determined were used to construct the footprinting plots.

Figure 6 shows a collection of footprinting plots corresponding to each CpG step present in the inserts CB1, CB2, and CB3. In every case, the cleavage intensity decreases rapidly with increasing echinomycin concentration. The decrease reflects the direct effect of the DNA-bound antibiotic molecules which impede access of DNase I to the CpG sites. Each plot reflects the fractional saturation at a given CpG site, but the fractional saturation is not equal to *R* because the plateau value at high antibiotic concentration is manifestly not on the abscissa ($R = 0$), and it varies from site to site. The asymptote at high *c* is determined by the effectiveness of bound antibiotic at inhibiting DNA cleavage which may be wholly unrelated to its thermodynamic binding constant as previously discussed (Goodisman & Dabrowiak, 1992; Sayers & Waring, 1993). It is the C_{50} value, the drug concentration required for half-maximal footprinting, which holds the thermodynamic data, and the important question is how such information may best be harvested.

The plots were fitted satisfactorily according to eq 1 or 2 described in the Materials and Methods section. C_{50} values were automatically measured from the fitting procedure (calculated from the parameter C in eqs 1 and 2). The C_{50} values determined for each CpG step within the three insert sequences vary markedly depending on both the sequence of the recognition site and the distance between the two CpG steps, as illustrated graphically in Figure 7. With each insert, the C_{50} value at the TCGA site is much higher than that at the neighboring ACGT site, indicating that echinomycin prefers the latter type of site having a purine−pyrimidine alternation over the former type of site. The C_{50} at the TCGA site is significantly lower when the nearest ACGT site is directly juxtaposed to it (CB3) rather than when the TCGA and ACGT sites are separated by two or four A·T bp. The same is true for the two closely spaced ACGT sites: the C_{50} values determined for both CpG steps in the sequence A<u>CG</u>T$(A{\cdot}T)_2$A<u>CG</u>T are significantly reduced when there are only two intervening A·T bp and are further diminished when the two sites are directly adjacent.

An alternative procedure to estimate binding affinities of echinomycin for each CpG-containing site consists in measuring the initial slopes of the footprinting plots. The affinity of the drug for a given site is inversely proportional to the relative slope of the plot: the more negative the slope, the higher the affinity constant of the antibiotic for a given binding site (Dabrowiak et al., 1989; Stankus et al., 1992; Shubsda et al., 1994). The results shown in Figure 8 agree perfectly with those in Figure 7 insofar as the binding of echinomycin at an A<u>CG</u>T site is facilitated when a second site, A<u>CG</u>T or T<u>CG</u>A, is adjacent to the first site. The relative slope of the footprinting plot for echinomycin binding to A<u>CG</u>T becomes more negative when the distance between the two contiguous A<u>CG</u>T sites diminishes. Similarly, the relative slope at T<u>CG</u>A is more negative when the T<u>CG</u>A site is directly adjacent to A<u>CG</u>T than when the two sites are separated by two or four A·T bp. Cooperative binding to GC sites can evidently be exploited by echinomycin to increase the occupancy at the weaker site TCGA. Both Figures 7 and 8 concur that the occupation of one CpG-containing site by echinomycin increases the binding affinity at an adjacent CpG site for the second echinomycin molecule. That the extent of cooperativity differs for adjacent ACGT and TCGA sites suggests a role for the sequence-dependent conformation of DNA.

Effects of Echinomycin on AT Sequences Flanking Strong Binding Sites. It can be seen in the control lanes of Figure 3 that the DNase I cleavage within the alternating $(AT)_n$ sequences consists of an alternating pattern of bands with strong cleavage at ApT and little or no cleavage at TpA, as previously reported by others (Suggs & Wagner 1986; McClellan et al., 1986; Fox, 1992). The data in Figure 3

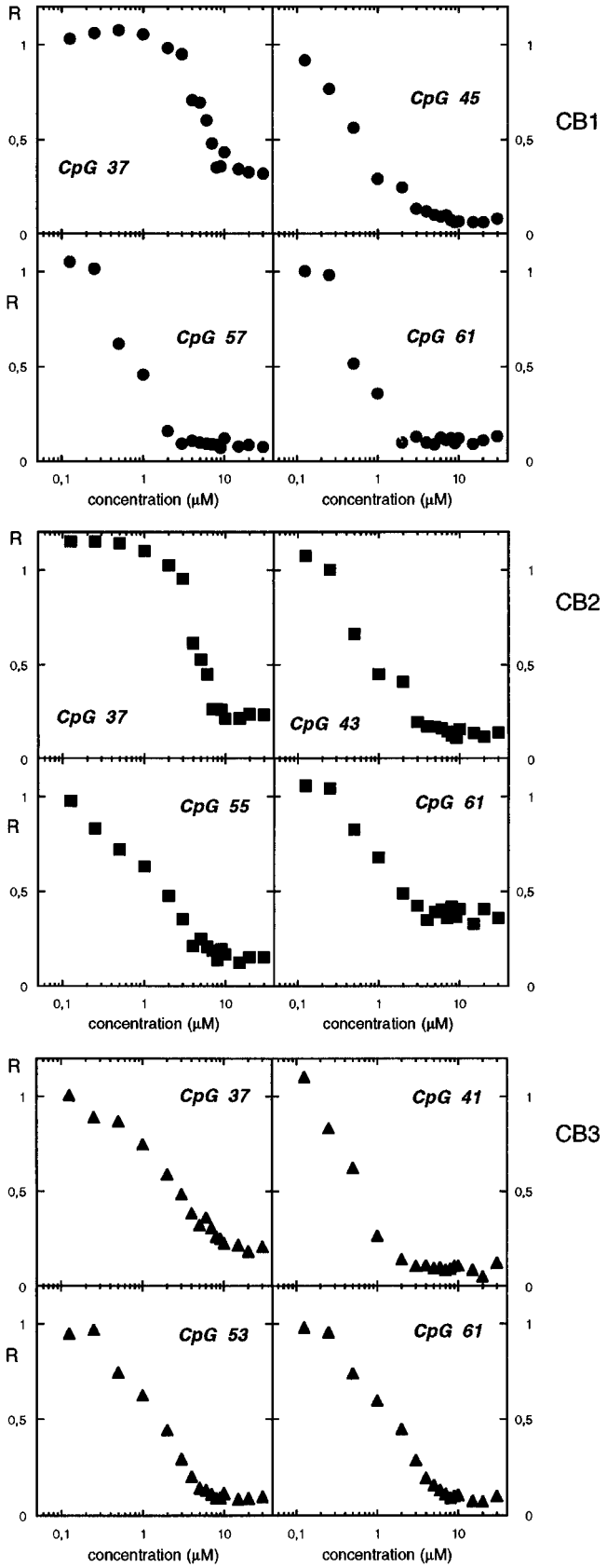

FIGURE 6: Footprinting plots for each of the four CpG bonds present in the CB1, CB2 and CB3 plasmid sequences. The relative band intensity R corresponds to the ratio I_c/I_o, where I_c is the intensity of the band at the ligand concentration c and I_o is the intensity of the same band in the absence of the antibiotic. Data points were obtained from gels such as those shown in Figure 3.

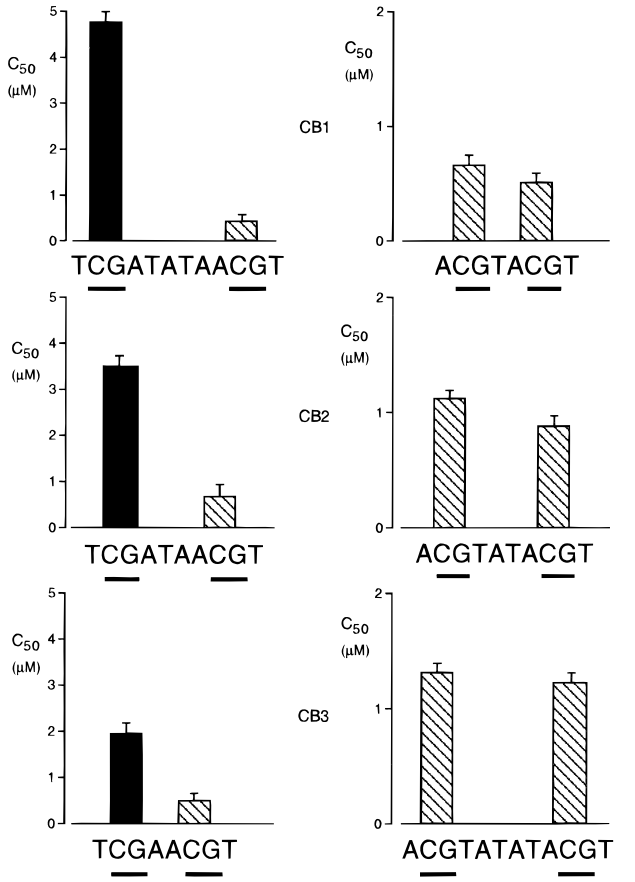

FIGURE 7: Variation of the C_{50} value (drug concentration required for half-maximal footprinting) at each CpG step within the three insert sequences. Under the conditions of these footprinting experiments, a large proportion of the added echinomycin molecules is likely to remain free, such that C_{50} values will approximate to thermodynamic dissociation constants for binding to individual sites (Dabrowiak & Goodisman, 1989). Data are given as mean ± standard error.

support a previous conclusion (Fox & Kentebe, 1990; Waterloh & Fox, 1991; Fox et al., 1991) that in the presence of echinomycin the cleavage at TpA steps increases considerably whereas cleavage at ApT steps is little affected. Not all ApT and TpA steps exhibit the same susceptibility to DNase I attack in the presence of echinomycin. Footprinting plots for selected TpA and ApT steps within each insert are presented in Figure 9. In several instances (e.g., ApT 31 and 66), the relative band intensity R increases with increasing echinomycin concentration (the initial slope is positive). Increases in the cleavage rate of the enzyme are often observed in footprinting experiments with drugs, especially with echinomycin (Sayers & Waring, 1993; Bailly & Waring, 1995b). Enhancements most likely occur as a result of the large-scale local deformation of the double helix (48° unwinding, stiffening, and lengthening of the sugar−phosphate backbone by 6.8 Å per echinomycin molecule) induced by bis-intercalation of the antibiotic into DNA (Waring, 1979). Echinomycin-induced distortion of $(A{\cdot}T)_n$ stretches flanking the site of bis-intercalation has been reported (Fox & Kentebe, 1990). Long-range structural distortions of DNA remote from the site of intercalation are also frequently observed with monointercalating drugs such as proflavine (Neidle & Abraham, 1984; Neidle et al., 1987). Although enhanced nuclease cleavage is usually interpreted as arising from ligand-induced structural changes, there are two alternative explanations for the enhanced cutting observed: (a) attractive interaction between the nuclease and

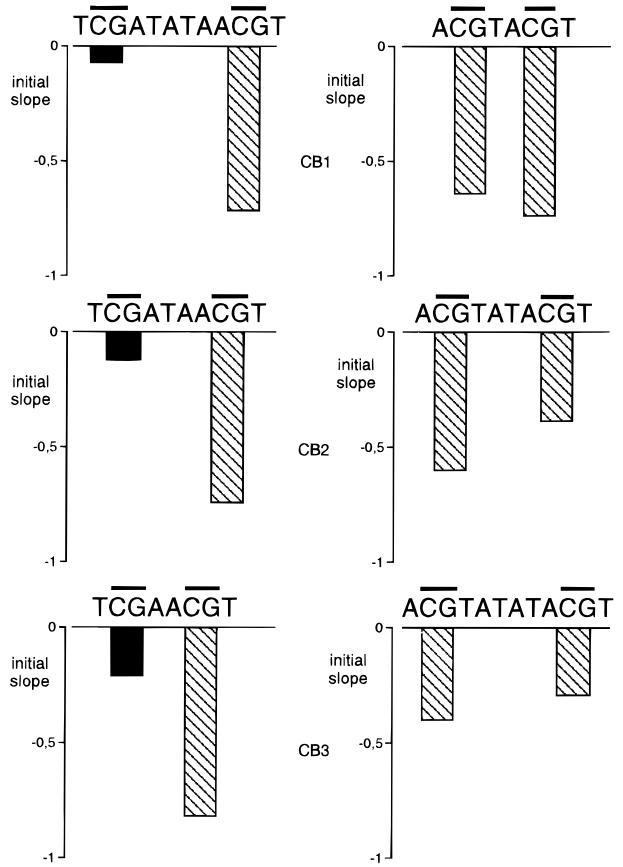

FIGURE 8: Variation of the initial slope of footprinting plots for the CpG steps. The initial slopes were determined as indicated in Materials and Methods.

the drug, leading to locally increased DNase I concentration around the drug-binding sites and (b) a mass-action effect, due to drug-induced displacement of the nuclease away from the drug-binding sites and resultant increase of the effective nuclease concentration at other sites not recognized by the drug (Ward et al., 1988; Goodisman & Dabrowiak, 1992). The elevated DNase I cutting at particular AT sites may originate from some combination of all three explanations.

At several positions, such as TpA 51 in CB1 and CB2, the rate of cleavage of the phosphodiester bonds in the AT sequence shows little variation with increasing echinomycin concentration. Just as we argued in the case of enhanced cleavage, this surely reflects the inability of echinomycin to bind to the $(A{\cdot}T)_n$ tracts flanking the CpG sites. In fact, $(A{\cdot}T)_n$ stretches are often refractory to intercalative drug binding. However, Fox and co-workers have suggested that echinomycin can bind in a cooperative manner to a dinucleotide step ApT embedded in an alternating AT sequence provided that the ApT site is proximal to a GC core (Fox et al., 1991; Waterloh & Fox 1991). In the present study, we have observed a weak but noticeable footprint at positions 24−26 (Figures 3 and 4), i.e., near the junction between the $(AT)_n$ tract and the very GC-rich sequence which lies just outside the insert (Figure 2). At first sight it is tempting to speculate that this footprint, which occurs at the same position and to roughly the same extent with each insert, reflects the binding of echinomycin to a pure AT site. However, the footprint is detected only on the 5′-labeled strand of the inserted sequence. As shown in Figure 9, the rate of cleavage at position TpA 24 decreases with increasing

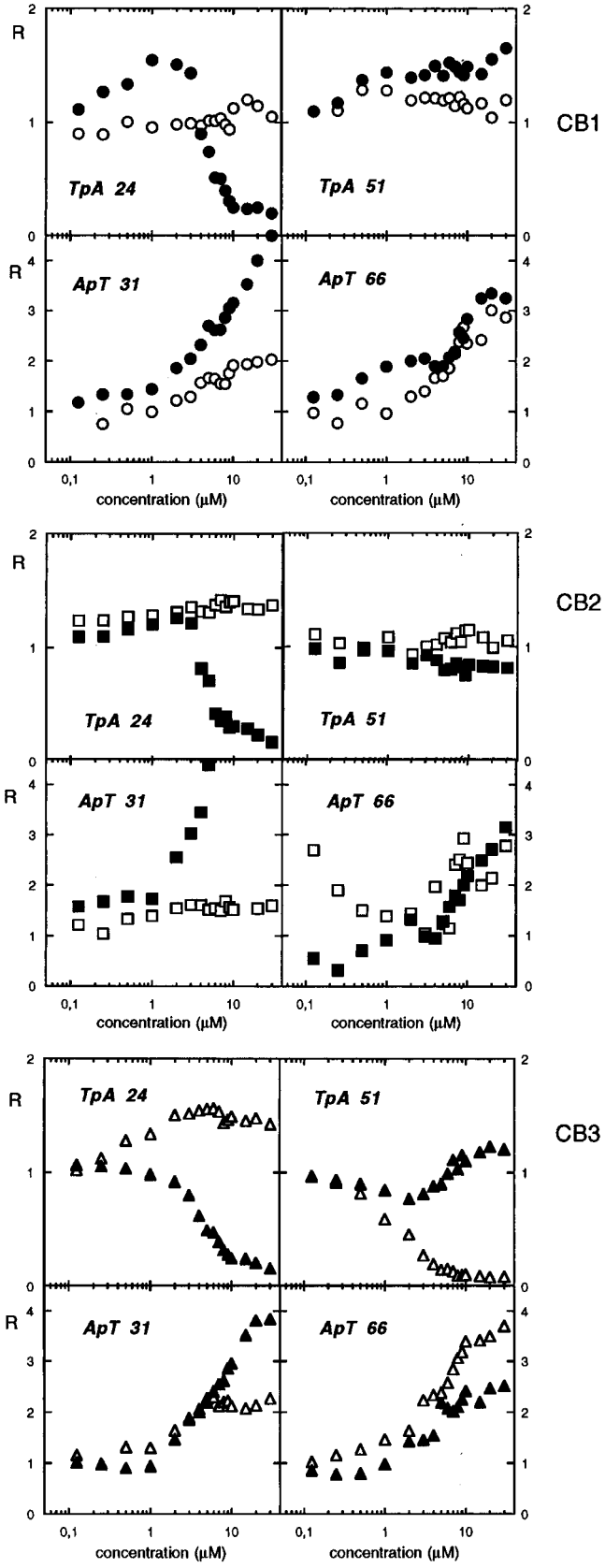

FIGURE 9: Footprinting plots for selected TpA and ApT bonds in the CB1, CB2, and CB3 sequences. Open and filled symbols refer, respectively, to the 3′- and 5′-labeled strands of the DNA fragment. Other details are as for Figure 6.

echinomycin concentration when the DNA is labeled on the 5′-end but increases slightly when the DNA is labeled on the complementary strand (3′-end labeling). For this reason, we prefer to believe that the apparently one-sided footprint

at this particular AT site does not indicate a secondary binding site for echinomycin but rather results from a peculiar local perturbation of the helix which slightly inhibits access of the enzyme to one strand. Furthermore, no hypersensitivity to chemical probes such as DEPC and OsO_4 was detected at this AT site (data not shown) whereas binding of echinomycin to GC sites renders the bases adjacent to the clamped step very susceptible to DEPC attack (Mendel & Dervan, 1987; Portugal et al., 1988; Bailly et al., 1994; Bailly & Waring, 1995b). However, the origin of the weak footprint at the AT site around positions 24−26 does remain enigmatic.

DISCUSSION

Quantitative DNase I footprinting has been used to determine the strength of binding to specific nucleotide sequences of drugs such as netropsin and distamycin (Fish et al., 1988; Ward et al., 1987, 1988), actinomycin D (Rehfuss et al., 1990; Goodisman et al., 1992), chromomycin (Stankus et al., 1992), daunomycin (Chaires et al., 1990), and echinomycin (Sayers & Waring, 1993). The methodology has also been exploited with signal success to investigate the cooperative binding of proteins to DNA (Senear et al., 1986; Brenowitz et al., 1993), but, so far as we are aware, this study is the first one in which the methodology has been applied to evidence the cooperative binding to DNA of a low molecular weight drug. Although different methods can be used to adduce evidence for the existence of cooperativity in drug binding to DNA, only a few can provide information pertaining to different sites within a single DNA fragment. For example, NMR spectroscopy has been used to investigate the cooperative binding of echinomycin to DNA, but the analysis is limited by the need to use short (8−12 bp) oligonucleotides and it demands rather large quantities of antibiotic and DNA. The great advantage of the footprinting titration experiment is the detailed view of the binding behavior which it reveals at several sites within a relatively long DNA fragment. The method allows us to examine the binding of the drug simultaneously at each bond in DNA and thus to estimate the relative strength of interaction with different binding sites within the same DNA molecule. Placement of the sites distal or proximal to each other does not hinder the measurements but, by contrast, permits us to evaluate the extent of cooperativity in the DNA binding reaction.

Prior to discussing the results, it is appropriate to draw attention to the mathematical procedure used to fit the footprinting plots. Analysis of the interaction between echinomycin and multiple or adjacent binding sites would ideally require consideration of a complex binding model incorporating specific parameters to describe cooperativity or anticooperativity (e.g., mutual exclusion between adjacent binding sites). In such circumstances, it is not an easy task to define appropriate equations which include all the necessary parameters in the correct functional form. Although binding expressions which refer to two and more ligand binding sites on DNA have been formulated [discussed in Dabrowiak and Goodisman, (1989) and in Brenowitz et al. (1993)], the equations are rather complex and not easily accessible to the nonspecialist. Therefore, to simplify the numerical analysis, we adopted the binding expressions 1 and 2 derived from a conventional statistical−mechanical approach. These equations as used in the present study may not represent the exact binding configuration but the approach is straightforward and applicable to a variety of situations whatever the number and arrangement of drug-binding sites on DNA. Accordingly the system employed here has the virtue of practicality and should prove useful to other workers.

The quantitative footprinting analysis reported here establishes unequivocally that binding of echinomycin to DNA is a sequence-specific and occasionally cooperative molecular recognition process. The results provide strong evidence for a high degree of cooperativity in the binding of the antibiotic to certain closely spaced ACGT and TCGA sites. As such, our findings fully agree with the NMR studies of echinomycin binding to the sequences ACGTACGT (Gilbert & Feigon, 1991) and ACGTATACGT (Gilbert & Feigon, 1992) where a cooperative interaction between antibiotic molecules bound to each of the CpG steps was evidenced. Whereas the NMR analysis showed no cooperativity between echinomycin molecules bound to TCGATCGA (Gilbert & Feigon, 1991), we show here that cooperative interaction can be detected when echinomycin binds to the sequence TCGAACGT.

The extent of cooperativity depends on both the sequence of the antibiotic binding sites and the distance between those sites. Satisfying though that conclusion may be, it leaves unresolved the question of the origin of the cooperativity. It might result either from direct ligand−ligand interactions or as the product of an altered DNA conformation induced by the binding of the drug. Both mechanisms are likely to be influenced by the spacing between the CpG sites and the sequences neighboring the CpG steps. Given both the NMR and footprinting data, it is unlikely that the cooperativity originates from direct interaction between contiguously-bound echinomycin molecules. Considering the observation that the cooperativity is sequence-dependent, we are inclined to believe, as surmised from previous equilibrium binding studies (Fox et al., 1982), that the cooperativity arises primarily as a result of a drug-induced progressive perturbation of the DNA helix. We have recently reported experiments indicating that DNA conformation plays a determinant role in regulating drug−DNA recognition (Bailly & Waring, 1995a,c; Bailly et al., 1995). Cooperativity mediated via conformational changes in DNA has been envisaged with monointercalating drugs such as daunomycin (Krugh et al., 1981; Chaires, 1983; Correia & Chaires, 1994), ethidium (Winkle et al., 1982), actinomycin, and certain anthracenedione derivatives. Cooperative binding of distamycin and DAPI into the minor groove of DNA and synthetic polynucleotides has also been reported (Samuelson et al., 1994). It is entirely possible that cooperative binding of drugs to DNA may be an underlying principle for enhancing their effect on DNA structure and metabolism.

Echinomycin is engaged in direct contacts only with the central CpG dinucleotide step in TCGA and ACGT sequences. However, the present study reinforces the view that the flanking A·T bp, which can only contact the quinoxaline rings of the antibiotic via stacking interactions, is involved in the drug−DNA recognition process. It seems clear that both direct and indirect reading of the DNA are necessary components of the cooperative, site-specific interaction between echinomycin and its receptor sites. It remains to be determined what structural elements in DNA

contribute to the sequence-dependent cooperative binding process. In recent studies we showed that, on the one hand, echinomycin (in common with numerous other antibiotics) is extremely sensitive to the relocation of the 2-amino group of guanine in DNA (Bailly & Waring, 1995a) and that, on the other hand, the exocyclic amino substituent on guanosines plays a critical role in governing DNA structure: in particular it seems to regulate the width of the minor groove (Bailly et al., 1995). On the basis of these observations, it is tempting to propose that the facilitated binding of echinomycin at the TCGA site in the sequence TCGAACGT arises, at least in part, from the change in the minor groove width at this site induced by the clamping of the adjacent CpG step. Bis-intercalation of echinomycin around a CpG step induces significant structural changes in the DNA helix. These changes are different for TCGA and ACGT oligonucleotides since upon binding of echinomycin the A·T bp on the 5′-side of the CpG step remains Watson−Crick paired in the TCGA complex but becomes Hoogsteen paired in the ACGT complex. The Watson−Crick → Hoogsteen base-pairing transition is presumed to reflect different intermolecular stacking interaction between the quinoxaline chromophore and the adenosine ring (Gao & Patel, 1988). If the same difference in stacking is apt to occur in DNA, it is plausible to believe that the unwinding and concomitant changes in minor groove width are also slightly different. These structural changes at the primary binding site may propagate differently to the second site and hence may be differently perceived by the second echinomycin molecule intercalating nearby.

In all events, the present results serve to indicate the general utility of quantitative footprinting as a means of establishing cooperativity in drug binding to DNA according to our experimental design. For some purposes it could be simplified by merely comparing, within a chosen DNA fragment, the binding to an internal "control" site with the binding to a couple of identical sites judiciously spaced by a neutral sequence like the ones we have studied here.

Although we do not fully understand the factors responsible for the cooperativity, it is likely that the phenomena associated with cooperative binding of echinomycin and other antitumor antibiotics to DNA are important in the therapeutic activity of these substances. Synergy could be enhanced further, or prevented, by interaction of the target sequences with other drugs. Quantitative footprinting may thus prove useful as a means to evaluate the effects of drugs used in combination chemotherapy.

ACKNOWLEDGMENT

We thank Dean Gentle for his invaluable technical assistance and are especially grateful to Dr. J. M. Smith and Sir Aaron Klug for providing access to the GELTRAK program operated within the computing facilities of the Medical Research Council Laboratory of Molecular Biology, Hills Road, Cambridge. C.B. thanks Dr. J. F. Goossens for the use of the program Kaleidagraph.

REFERENCES

Addess, K. J., & Feigon, J. (1994a) *Biochemistry 33*, 12386−12396.
Addess, K. J., & Feigon, J. (1994b) *Biochemistry 33*, 12397−12404.
Addess, K. J., & Feigon, J. (1994c) *Nucleic Acids Res. 22*, 5484−5491.
Bailly, C., & Waring, M. J. (1995a) *Nucleic Acids Res. 23*, 885−892.
Bailly, C., & Waring, M. J. (1995b) *J. Biomol. Struct. Dyn. 12*, 869−898.
Bailly, C., & Waring, M. J. (1995c) *J. Am. Chem. Soc. 117*, 7311−7316.
Bailly, C., Marchand, C., & Waring, M. J. (1993) *J. Am. Chem. Soc. 115*, 3784−3785.
Bailly, C., Gentle, D., Hamy, F., Purcell, M., & Waring, M. J. (1994) *Biochem. J. 300*, 165−173.
Bailly, C., Møllegaard, N. E., Nielsen, P. E., & Waring, M. J. (1995) *EMBO J. 14*, 2121−2131.
Brenowitz, M., Senear, D., Jamison, E., & Dalma-Weiszhausz, D. (1993) in *Footprinting of Nucleic Acid−Protein Complexes* (Revzin, A., Ed.) pp 1−43, Academic Press, Inc., San Diego, CA.
Chaires, J. B. (1983) *Biochemistry 22*, 4204−4211.
Chaires, J. B., Herrera, J. E., & Waring, M. J. (1990) *Biochemistry 29*, 6145−6153.
Correia, J. J., & Chaires, J. B. (1994) *Methods Enzymol. 240*, 593−614.
Dabrowiak J. C., & Goodisman J. (1989) in *Chemistry and Physics of DNA−Ligand Interactions* (Kallenbach, N. R., Ed.) pp 143−174, Adenine Press, Guilderland, NY.
Dabrowiak J. C., Kissinger, K., & Goodisman J. (1989) *Electrophoresis 10*, 404−412.
Fish, E. L., Lane, M. J., & Vournakis, J. N. (1988) *Biochemistry 27*, 6026−6032.
Fox, K. R. (1992) *Nucleic Acids Res. 20*, 6487−6493.
Fox, K. R., & Kentebe (1990) *Nucleic Acids Res. 18*, 1957−1963.
Fox, K. R., Wakelin, L. P. G., & Waring, M. J. (1981) *Biochemistry 20*, 5768−5779.
Fox, K. R., Olsen, R. K., & Waring, M. J. (1982) *Biochim. Biophys. Acta 696*, 315−322.
Fox, K. R.. Marks, J. N., & Waterloh, K. (1991) *Nucleic Acids Res. 19*, 6725−6730.
Gao, X., & Patel, D. J. (1988) *Biochemistry 27*, 1744−1751.
Gao, X., & Patel, D. J. (1989) *Q. Rev. Biophys. 22*, 93−138.
Gilbert, D. E., & Feigon, J. (1991) *Biochemistry 30*, 2483−2494.
Gilbert, D. E., & Feigon, J. (1992) *Nucleic Acids Res. 20*, 2411−2420.
Goodisman, J., & Dabrowiak, J. C. (1992) *Biochemistry 31*, 1058−1064.
Goodisman, J., Rehfuss, R., Ward, B., & Dabrowiak, J. C. (1992) *Biochemistry 31*, 1046−1058.
Johnston, R. F., Pickett, S. C., & Barker, D. L. (1990) *Electrophoresis 11*, 355−360.
Krugh, T. R., Winkle, S. A., & Graves, D. E. (1981) *Biochem. Biophys. Res. Commun. 98*, 317−323.
Lee, J. S., & Waring, M. J. (1978) *Biochem. J. 173*, 129−144.
Leroy, J. L., Gao, X., Misra, V., Guéron, M., & Patel, D. J. (1992) *Biochemistry 31*, 1407−1415.
Low, C. M. L., Drew, H. R., & Waring, M. J. (1984) *Nucleic Acids Res. 12*, 4865−4879.
Marchand, C., Bailly, C., McLean, M. J., Moroney, S., & Waring, M. J. (1992) *Nucleic Acids Res. 21*, 5601−5606.
McClellan, J. A., Palecek, E., & Lilley, D. (1986) *Nucleic Acids Res. 14*, 9291−9309.
Mendel, D., & Dervan, P. B. (1987) *Proc. Natl. Acad. Sci. U.S.A. 84*, 910−914.
Neidle, S., & Abraham, Z. (1984) *Crit. Rev. Biochem. 17*, 73−121.
Neidle, S., Pearl, L. H., & Skelly, J. V. (1987) *Biochem. J. 243*, 1−13.
Portugal, J., Fox, K. R., McLean, M. J., Richenberg, J. L., & Waring, M. J. (1988) *Nucleic Acids Res. 16*, 3655−3670.
Quigley, G. J., Ughetto, G., van der Marel, G. A., van Boom, J. H., Wang, A. H.-J., & Rich, A. (1986) *Science 232*, 1255−1258.
Rehfuss, R., Goodisman, J., & Dabrowiak, J. C. (1990) *Biochemistry 29*, 777−781.
Samuelson, P., Jansen, K., Kubista, M. (1994) *J. Mol. Recognit. 7*, 233−241.

Sayers, E. W., & Waring, M. J. (1993) *Biochemistry 32*, 9094−9107.
Senear, D. F., Brenowitz, M., Shea, M. A., & Ackers, G. K. (1986) *Biochemistry 25*, 7344−7354.
Shafer, R. H., & Waring, M. J. (1982) *Biopolymers 21*, 2279−2290.
Shubsda, M., Kishikawa, H., Goodisman, J., & Dabrowiak, J. (1994) *J. Mol. Recognit. 7*, 133−139.
Smith, J. M., & Thomas, D. J. (1990) *Comput. Appl. Biosci. 6*, 93−99.
Stankus, A., Goodisman, J., & Dabrowiak, J. C. (1992) *Biochemistry 31*, 9310−9318.
Suggs, J. W., & Wagner R. W. (1986) *Nucleic Acids Res. 14*, 3703−3716.
Ughetto, G., Wang, A. H.-J., Quigley, G. J., van der Marel, G. A., van Boom, J. H., & Rich, A. (1984) *Nucleic Acids Res. 13*, 2305−2323.
Van Dyke, M. W., & Dervan, P. B. (1984) *Science 225*, 1122−1127.
Wang, A. H.-J., Ughetto, G., Quigley, G. J., Hakoshima, T., van der Marel, G. A., van Boom, J. H., & Rich, A. (1984) *Science 225*, 1115−1121.
Ward, B., Rehfuss, R., & Dabrowiak, J. C. (1987) *J. Biomol. Struct. Dyn. 4*, 685−695.
Ward, B., Rehfuss, R., Goodisman, J., & Dabrowiak, J. C. (1988) *Biochemistry 27*, 1198−1205.
Waring, M. J. (1979) in *Antibiotics*: *Mechanism of Action of Antieukaryotic and Antiviral Compounds* (Hahn, F. E., Ed.), Vol. 5, Part 2, pp 173−194, Springer-Verlag, Heidelberg.
Waring, M. J. (1993) in *Molecular Aspects of Anticancer Drug−DNA Interactions* (Neidle, S., & Waring, M. J., Eds.) Vol. 1, pp 213−242, Macmillan, London.
Waring, M. J., & Wakelin, L. P. G. (1974) *Nature (London) 252*, 653−657.
Waterloh, K., & Fox, K. R. (1991) *Nucleic Acids Res. 19*, 6719−6724.
Winkle, S. A., Rosenberg, L. S., & Krugh, T. R. (1982) *Nucleic Acids Res. 10*, 8211−8223.

BI951696P